Measurement of small light absorption in microparticles by means of optically induced rotation

Angelsky, O. V.; Bekshaev, A. Ya; Maksimyak, P. P.; Maksimyak, A. P.; Hanson, Steen Grüner

Published in:
Optics Express

Link to article, DOI:
10.1364/OE.23.007152

Publication date:
2015

Document Version
Publisher's PDF, also known as Version of record

Measurement of small light absorption in microparticles by means of optically induced rotation

O. V. Angelsky,[1]* A. Ya. Bekshaev,[2] P. P. Maksimyak,[1] A. P. Maksimyak,[1] and S. G. Hanson[3]

[1]*Correlation Optics Department, Chernivtsi National University, 2, Kotsyubinsky Str., Chernivtsi 58012, Ukraine*
[2]*Research Institute of Physics, Odessa I.I. Mechnikov National University, Dvorianska 2, Odessa 65082, Ukraine*
[3]*DTU Fotonik, Department of Photonics Engineering, DK-4000 Roskilde, Denmark*
[*]*angelsky@itf.cv.ua*

Abstract: The absorption parameters of micro-particles have been associated with the induced spin exerted upon the particle, when embedded in a circularly polarized coherent field. The induced rotational speed is theoretically analyzed, showing the influence of the beam parameters, the parameters of the particle and the tribological parameters of the surrounding fluid. The theoretical findings have been adequately confirmed in experiments.

OCIS codes: (260.2160) Energy transfer; (260.5430) Polarization; (350.4855) Optical tweezers or optical manipulation; (350.4990) Particles.

References and links

1. C. F. Bohren and D. R. Huffman, *Absorption and Scattering of Light by Small Particles* (Wiley,1983).
2. A. Ashkin, "Applications of laser radiation pressure," Science **210**(4474), 1081–1088 (1980).
3. A. Ashkin, "Optical trapping and manipulation of neutral particles using lasers," Proc. Natl. Acad. Sci. U.S.A. **94**(10), 4853–4860 (1997).
4. M. Dienerowitz, M. Mazilu, and K. Dholakia, "Optical manipulation of nanoparticles: a review," J. Nanophoton. **2**(1), 021875 (2008).
5. O. V. Angelsky, M. P. Gorsky, P. P. Maksimyak, A. P. Maksimyak, S. G. Hanson, and C. Yu. Zenkova, "Investigation of optical currents in coherent and partially coherent vector fields," Opt. Express **19**(2), 660–672 (2011).
6. O. V. Angelsky, A. Ya. Bekshaev, P. P. Maksimyak, A. P. Maksimyak, S. G. Hanson, and C. Yu. Zenkova, "Orbital rotation without orbital angular momentum: mechanical action of the spin part of the internal energy flow in light beams," Opt. Express **20**(4), 3563–3571 (2012).
7. O. V. Angelsky, A. Ya. Bekshaev, P. P. Maksimyak, A. P. Maksimyak, S. G. Hanson, and C. Yu. Zenkova, "Self-diffraction of continuous laser radiation in a disperse medium with absorbing particles," Opt. Express **21**(7), 8922–8938 (2013).
8. A. I. Bishop, T. A. Nieminen, N. R. Heckenberg, and H. Rubinsztein-Dunlop, "Optical application and measurement of torque on microparticles of isotropic nonabsorbing material," Phys. Rev. A **68**(3), 033802 (2003).
9. K. S. Lee and M. A. El-Sayed, "Gold and silver nanoparticles in sensing and imaging: sensitivity of plasmon response to size, shape, and metal composition," J. Phys. Chem. B **110**(39), 19220–19225 (2006).
10. J. Xia, J. Yao, and L. H. V. Wang, "Photoacoustic tomography: principles and advances (invited review)," Prog. Electromagnetics Res. **147**, 1–22 (2014).
11. K. Svoboda and S. M. Block, "Biological applications of optical forces," Annu. Rev. Biophys. Biomol. Struct. **23**(1), 247–285 (1994).
12. R. A. Freitas, "Current status of nanomedicine and medical nanorobotics," J. Comp. Theo. Nanosci. **2**, 1–25 (2005).
13. E. J. Davis and G. Schweiger, *The Airborne Microparticle: Its Physics, Chemistry, Optics, and Transport Phenomena* (Springer, 2002).
14. J. A. Burns, P. L. Lamy, and S. Soter, "Radiation forces on small particles in the solar system," Icarus **40**(1), 1–48 (1979).
15. T. Henning, "Interstellar dust grains – An overview," Molecules in Astrophysics: Probes and Processes **178**, 343–356 (1997).

#231377 - $15.00 USD Received 12 Jan 2015; revised 25 Feb 2015; accepted 25 Feb 2015; published 9 Mar 2015

16. A. B. Pluchino, S. S. Goldberg, J. M. Dowling, and C. M. Randall, "Refractive-index measurements of single micron-sized carbon particles," Appl. Opt. **19**(19), 3370–3372 (1980).
17. P. J. Wyatt, "Some chemical, physical, and optical properties of fly ash particles," Appl. Opt. **19**(6), 975–983 (1980).
18. P. Chylek, V. Ramaswamy, A. Ashkin, and J. M. Dziedzic, "Simultaneous determination of refractive index and size of spherical dielectric particles from light scattering data," Appl. Opt. **22**(15), 2302–2307 (1983).
19. M. Nieto-Vesperinas, J. J. Sáenz, R. Gómez-Medina, and L. Chantada, "Optical forces on small magnetodielectric particles," Opt. Express **18**(11), 11428–11443 (2010).
20. P. L. Marston and J. H. Crichton, "Radiation torque on a sphere caused by a circularly polarized electromagnetic wave," Phys. Rev. A **30**(5), 2508–2516 (1984).
21. S. Chang and S. S. Lee, "Optical torque exerted on a homogeneous sphere levitated in the circularly polarized fundamental-mode laser beam," J. Opt. Soc. Am. B **2**(11), 1853–1860 (1985).
22. J. S. Kim and S. S. Lee, "Scattering of laser beams and the optical potential well for a homogeneous sphere," J. Opt. Soc. Am. **73**(3), 303–312 (1983).
23. S. M. Barnett and R. Loudon, "The enigma of optical momentum in a medium," Philos Trans A Math Phys Eng Sci **368**(1914), 927–939 (2010).
24. I. Brevik, "What do experiments in optics tell us about photon momentum in media?" Preprint at http://arxiv.org/abs/1310.3684v1 (2013).
25. A. Y. Bekshaev, K. Y. Bliokh, and F. Nori, "Mie scattering and optical forces from evanescent fields: a complex-angle approach," Opt. Express **21**(6), 7082–7095 (2013).
26. M. Abramovitz and I. Stegun, eds., *Handbook of Mathematical Functions*, National Bureau of Standards, Applied Mathematics Series **55**, 1964.
27. A. Y. Bekshaev, "Subwavelength particles in an inhomogeneous light field: optical forces associated with the spin and orbital energy flows," J. Opt. **15**(4), 044004 (2013).
28. R. Gómez-Medina, B. García-Cámara, I. Suárez-Lacalle, F. González, F. Moreno, M. Nieto-Vesperinas, and J. J. Sáenz, "Electric and magnetic dipolar response of germanium nanospheres: interference effects, scattering anisotropy, and optical forces," J. Nanophoton. **5**(1), 053512 (2011).
29. B. T. Draine, "The discrete-dipole approximation and its application to interstellar graphite grains," Astrophys. J. **333**, 848–872 (1988).
30. T. A. Nieminen, V. L. Y. Loke, A. B. Stilgoe, G. Knoner, A. M. Branczyk, N. R. Heckenberg, and H. Rubinsztein-Dunlop, "Optical tweezers computational toolbox," J. Opt. A **9**(8), 196–203 (2007), http://www.physics.uq.edu.au/people/nieminen/software.html.
31. B. J. P. Jansen, K. Y. Tamminga, H. E. H. Meijer, and P. J. Lemstra, "Preparation of thermoset rubbery epoxy particles as novel toughening modifiers for glassy epoxy resins," Polymer (Guildf.) **40**(20), 5601–5607 (1999).
32. Atago Abbe Refractometer Model NAR-1T SOLID, User Manual (2010).
33. Model 6300, Visible Range Spectrophotometer, Operating Manual, *http://www.keison.co.uk/products/jenway/6300_6320_Manual.pdf*

1.Introduction

The problem of determining optical constants of micro- and nanoparticles [1] is very pertinent for numerous applications. The rapidly growing field of optical manipulation [2–4] offers efficient and promising means for fine chemical, biomedical and microelectronic technologies. Particles of different sizes and nature are widely used in detailed investigations of optical fields [5–7], enabling direct studies of microscopic properties of fluids and biological specimens such as viscosity or elasticity [8] as well as being the basis for many advanced research works that embrace a huge area from colloid chemistry and microbiology [9–12] to atmospheric aerosols and interstellar dust [13–15]. All these activities require, among other important physical information, knowledge of the particles' optical properties and their dependence on various external conditions.

In general, the well-known parameters of bulk materials are not applicable for very small quantities of the same substances [1]. Even in cases where the expected size-dependent factors are negligible, the specific conditions of small particles' formation may affect their chemical composition, structure, etc., and special procedures are necessary to validate the parameter values that regulate their optical behavior. In most cases, the sought optical constants are predominantly used for modeling of effects associated with light scattering, extinction and absorption by isolated particles and their ensembles. Consequently, special weight should be ascribed to techniques based on data for light scattering [16–18] – first of all, because the conditions under which the optical constants are measured, are close to the conditions for which they will be applied.

#231377 - $15.00 USD Received 12 Jan 2015; revised 25 Feb 2015; accepted 25 Feb 2015; published 9 Mar 2015

Within the frame of these techniques, the most powerful existing methods are based on comparison between experimental and theoretical data for the angular distribution of light scattered by an isolated particle relying on Mie scattering. In this case, the best fitting procedure gives a possibility to find the particle radius, real and imaginary parts of the refraction index and even the particle structure, provided that it is *a priori* known that the particle is spherical and consists of the 'core' and 'shell' with different optical properties [16,17]. These methods are comprehensive and informative. However, a large number of measured parameters usually obscure the fitting procedure and, quite typically, the minimum of a corresponding 'quality factor' (figure of merit) is imperfectly localized in the multidimensional parameter space. This calls for the search of less universal but more specialized methods aimed at some specific parameters whose influence on the scattering characteristics is more explicit and can be derived immediately. Possible ways for their realization are associated with the mechanical action of light on small particles, which, in fact, is nothing but a concentrated expression of some integral scattering characteristics [1,4,19–22].

Due to the intensive development of techniques for optical trapping and manipulation [4], it is presently not difficult to observe and to measure the characteristics of motion of a micro-particle suspended within an optical field. Such approaches provide suitable tools for evaluation of the mechanical ponderomotive factors (force and torque) which an optical field exerts on a particle. More importantly, the ponderomotive factors can be directly associated with the optical parameters of the particle, and this can be employed for their measurement.

For example, within the framework of the Mie theory [1], the optical force, *F*, and torque, *T*, exerted by a plane monochromatic wave on a homogeneous isotropic spherical particle, are directed along the wavevector and determined by the expressions

$$F=\frac{2\pi I}{k^2 c}n\sum_{\ell=1}^{\infty}\mathrm{Re}\left[(2\ell+1)(a_\ell+b_\ell)-\frac{2\ell(\ell+2)}{\ell+1}\left(a_\ell a_{\ell+1}^{*}+b_\ell b_{\ell+1}^{*}\right)-\frac{2(2\ell+1)}{\ell(\ell+1)}a_\ell b_\ell^{*}\right], \quad (1)$$

$$T=\frac{2\pi I}{k^2\omega}\sigma\sum_{\ell=1}^{\infty}(2\ell+1)\,\mathrm{Re}\left(a_\ell+b_\ell-|a_\ell|^2-|b_\ell|^2\right) \quad (2)$$

where I is the energy flow density in the wave, c is the light velocity in vacuum, ω is the wave frequency, $k=(\omega/c)n$ is its wavenumber, and σ is the wave spin number (normalized third Stokes parameter) equal to ± 1 for right (left) circular polarization and 0 for any linear or no polarization. Equations (1) and (2) differ from the analogous expressions of [1,20] in a single aspect: here the particle is assumed to be immersed in a homogeneous isotropic dielectric medium with real permittivity ε and real permeability μ so that the refraction index equals $n=\sqrt{\varepsilon\mu}$, and the multiplier n in Eq. (1) reflects the force amplification in an optically dense medium [23,24]. The symbols a_ℓ and b_ℓ denote the Mie scattering coefficients [1,25] dependent on the particle radius r via the dimensionless parameter $x=kr$ and given by

$$a_\ell=\frac{m_\varepsilon\psi_\ell(mx)\psi_\ell'(x)-m_\mu\psi_\ell(x)\psi_\ell'(mx)}{m_\varepsilon\psi_\ell(mx)\xi_\ell'(x)-m_\mu\xi_\ell(x)\psi_\ell'(mx)},\quad b_\ell=\frac{m_\mu\psi_\ell(mx)\psi_\ell'(x)-m_\varepsilon\psi_\ell(x)\psi_\ell'(mx)}{m_\mu\psi_\ell(mx)\xi_\ell'(x)-m_\varepsilon\xi_\ell(x)\psi_\ell'(mx)} \quad (3)$$

where

$$\xi_\ell(u)=u h_\ell^{(1)}(u),\ \xi_\ell'(u)=\frac{d\left[u h_\ell^{(1)}(u)\right]}{d(u)},\ \psi_\ell(u)=u j_\ell(u),\ \psi_\ell'(u)=\frac{d\left[u j_\ell(u)\right]}{du}, \quad (4)$$

#231377 - $15.00 USD Received 12 Jan 2015; revised 25 Feb 2015; accepted 25 Feb 2015; published 9 Mar 2015

$h_\ell^{(1)}(u)$ and $j_\ell(u)$ are the spherical Hankel and Bessel functions [26], respectively, and, for a particle with permittivity ε_p and permeability μ_p,

$$m_\varepsilon = \sqrt{\frac{\varepsilon_p}{\varepsilon}},\ m_\mu = \sqrt{\frac{\mu_p}{\mu}},\ m = \frac{n_p}{n} = \sqrt{\frac{\varepsilon_p\,\mu_p}{\varepsilon\,\mu}}.$$

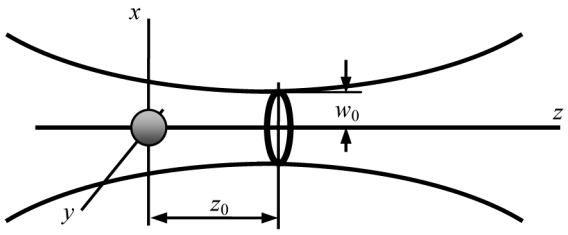

Fig. 1. Scattering of a Gaussian beam by an axially-trapped particle: the beam axis coincides with the axis z, and the particle centre is situated at a distance z_0 from the beam waist.

Despite their plane-wave origin, relations (1) and (2) are also applicable for inhomogeneous fields provided that the spatial scale of the inhomogeneity of the incident beam sufficiently exceeds the radiation wavelength and the particle size. This requirement is violated in typical optical-trapping situations where the particle is localized within a strongly focused laser beam with near-wavelength transverse size. Then the above equations should be modified. For example, if the particle is placed on the axis of a Gaussian beam (see Fig. 1), Eqs. (8) and (14) of [21] yield

$$T = \frac{|C|^2}{2k^3}\sigma\sum_{\ell=1}^{\infty}\frac{\ell^2(\ell+1)^2}{(2\ell+1)}\mathrm{Re}\left[|\alpha(\ell,1)|^2\left(b_\ell - |b_\ell|^2\right) + |\beta(\ell,1)|^2\left(a_\ell - |a_\ell|^2\right)\right], \qquad (5)$$

where the normalization constant $|C|^2$ can be expressed through the beam power P or the beam axial intensity $I_0 = 2P/\pi w_0^2$, w_0 being the waist radius measured at the e^{-1} amplitude level:

$$|C|^2 = \frac{8P}{w_0^2}\frac{\varepsilon}{cn\mu} = 4\pi I_0\frac{\varepsilon}{cn\mu}, \qquad (6)$$

and coefficients $\alpha(\ell,1)$, $\beta(\ell,1)$, first introduced in [21,22], originate from the Gaussian beam expansion in terms of the vector spherical wave functions. In Eq. (5) their normalization differs from that accepted in [21,22], which allowed them to be represented in rather simple forms:

$$\begin{aligned}\alpha(\ell,1) &= ipe^{-p}\frac{2\ell+1}{\ell(\ell+1)}h_\ell^{(1)}(-ip-kz_0),\\ \beta(\ell,1) &= pe^{-p}\frac{\ell h_{\ell+1}^{(1)}(-ip-kz_0) - (\ell+1)h_{\ell-1}^{(1)}(-ip-kz_0)}{\ell(\ell+1)},\end{aligned} \qquad (7)$$

with

$$p = \frac{1}{2}(kw_0)^2$$

#231377 - $15.00 USD Received 12 Jan 2015; revised 25 Feb 2015; accepted 25 Feb 2015; published 9 Mar 2015

and z_0 being the distance between the particle center and the beam waist (see Fig. 1). Quite expectedly, one can easily verify that in the limit $w_0 \to \infty$, when the spherical Hankel functions obey the asymptotic relations [26]

$$h_\ell^{(1)}(-ip) \xrightarrow[p\to\infty]{} \frac{e^p}{p}\exp\left(-i\ell\frac{\pi}{2}\right),$$

expression (5) reduces to Eq. (2) with the correspondence $I_0 \to I$.

Now we consider some features of expressions (1), (2) and (5) in more detail. Each of them contains the scattering coefficients a_ℓ and b_ℓ which represent the electric and magnetic 2^λ-multipole polarizabilities of the particle. In particular, the electric α_e and magnetic α_m dipole polarizabilities are related with the lowest-order coefficients,

$$a_1 = -i\frac{2k^3}{3\varepsilon}\alpha_e,\ b_1 = -i\frac{2k^3}{3\mu}\alpha_m. \tag{8}$$

Usually, the quantities (8) play a crucial role for small 'Rayleigh' particles with size much less than the radiation wavelength [19,27] but in some special cases their contributions may prevail even for considerably large particles [12]. Addressing Eqs. (2) and (5), one can see that, if the particle is non-absorbing (real ε_p and μ_p), quantities m_ε, m_μ and m are real, the numerators of expressions (3) equal the real parts of the denominators, so equalities $\mathrm{Re}\,a_\ell = |a_\ell|^2$ and $\mathrm{Re}\,b_\ell = |b_\ell|^2$ are true, and the particle experiences no torque ("the effective cross section for torque is the same as that for energy absorption" [20]). To analyze this property in more detail, we compare Eqs. (1) and (2) in the lowest-order approximation, keeping only the electric terms with $\lambda = 1$:

$$F = \frac{6\pi I}{k^2 c}\mathrm{Re}(a_1) = 4\pi I\frac{kn}{\varepsilon c}\mathrm{Im}(\alpha_e), \tag{9}$$

$$T = \frac{6\pi I}{k^2\omega}\sigma\,\mathrm{Re}\left(a_1 - |a_1|^2\right) = 4\pi I\frac{n}{\varepsilon c}\sigma\left(\mathrm{Im}(\alpha_e) - \frac{2k^3}{3\varepsilon}|\alpha_e|^2\right). \tag{10}$$

At first glance, the optical force being proportional to the imaginary part of the polarizability, appears due to the particle absorption. However, the imaginary contribution to the polarizability of non-absorbing particles can exist because of the radiation friction effect (self-action of the dipole induced by an incident field) [19,29] due to which

$$\alpha_e = \frac{\alpha_e^0}{1 - i\frac{2k^3}{3\varepsilon}\alpha_e^0} \approx \alpha_e^0 + i\frac{2k^3}{3\varepsilon}\left|\alpha_e^0\right|^2 \tag{11}$$

where α_e^0 is the 'static' polarizability corresponding to $k \to 0$ (the approximate equality (11) is valid for small dipole particles when $k^3\alpha_e^0 << 1$). In the Mie theory, this fact is reflected by the real part of the coefficient a_1 that emerges in higher orders of the expansion in degrees of x [1]. It is this 'reactive' contribution owing to the phase shift between the driving electric field and the field-induced dipole (both oscillating with frequency ω) that is responsible for the optical pressure on dielectric dipole particles [27].

On the contrary, torque is exactly zero for non-absorbing particles, which is directly illustrated by Eq. (10) with allowance for Eq. (11): the form of Eq. (10), and, of course, Eq. (2), is such that no "artificial" imaginarity associated with the phase difference between the

#231377 - $15.00 USD Received 12 Jan 2015; revised 25 Feb 2015; accepted 25 Feb 2015; published 9 Mar 2015

external electric field and the field-induced dipole moment affects the torque exerted on a particle. External spin acts on a spherical particle only if it is absorbed. Accordingly, the torque "felt" by a particle in a circularly polarized wave will facilitate the selective and sensitive measurement of the particle absorption.

Another advantage of using the field-induced torque as a preferential ponderomotive factor (compared to the optical force) is that a natural manifestation of any torque is the spinning motion of the particle whereas a force can be detected via its translations. This is usually coupled with more or less substantial displacement of a particle across an inhomogeneous field where the force varies from point to point making it difficult to establish an immediate correspondence between the force and the particle trajectory. Quite oppositely, the spinning particle typically preserves its position, or can be easily stabilized by means of routine optical trapping techniques, so that the field action is stable and well controllable.

2. Experiment

A schematic of the experimental equipment is presented in Fig. 2. A linearly polarized beam from the semiconductor laser 1 with wavelength λ = 0.65 μm and power P controllable with maximum 140 mW. The beam is collimated after the expander 2 with a pinhole filter to produce a Gaussian beam with a radius $w_i = 1.0$ mm measured at the intensity level e^{-2} of maximum. The quarter-wave plate 4 forms circular polarization, and the beam is focused by the micro-objective 5 with focal distance $f = 10$ mm which provides an effective focusing angle $\theta = \arctan\left(w_i / f\right) \approx 5.7°$. As a result, a Gaussian-shaped beam spot with a waist radius $w_0 \simeq 2f/\left(kw_i\right) \simeq 2.0$ μm is formed inside the cell 6, where the particles under test are suspended. Overall losses of the laser beam power in the system were estimated ~30% resulting in the maximum power in the cell to be ~100 mW.

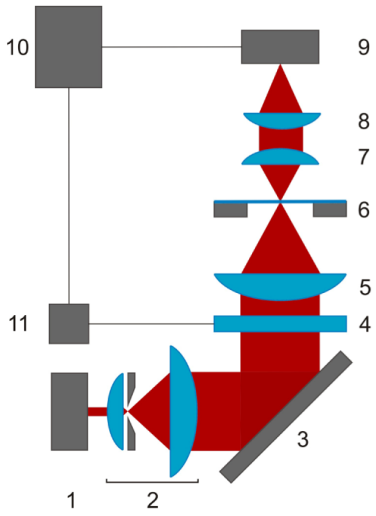

Fig. 2. Schematic of the experimental setup: (1) laser; (2) beam expander with spatial filter; (3) mirror; (4) quarter-wave plate; (5), (7) and (8) objective lenses; (6) cell with probing particles suspended in water; (9) CCD-camera; (10) personal computer; (11) control unit.

During the measurement, one of the suspended particles is trapped in the Gaussian beam's focal region. The motion of the particle is observed and registered by the projective system 7, 8 and CCD camera 9. The images are transmitted to the computer 10, which not only performs the image analysis and processing but also provides a possibility to control the laser power as well as the quarter-wave plate position and orientation via the control unit 11.

#231377 - $15.00 USD Received 12 Jan 2015; revised 25 Feb 2015; accepted 25 Feb 2015; published 9 Mar 2015

Several important conditions should be fulfilled in order that the field-induced spinning of suspended particles is observable and metrologically consistent. First, the viscosity of the suspending medium must be small enough; in the current experiments, distilled water was chosen with dynamical viscosity $\eta = 8.9 \cdot 10^{-3}$ dyn·s·cm^{-2} (at 25°C). Second, refracting particles (with low reflection) are preferable because these will be trapped within the maximum of the Gaussian beam implying that the particle refraction index n_p exceeds that of water $n = 1.33$. For efficient concentration of the laser beam energy onto the particle, strong focusing with a high-NA objective is desirable. However, in this case the measurement process becomes sensitive to small deviations of the beam-waist size w_0 from the nominal value; this is why the moderate-strength focusing micro-objective is employed. Further, requirement of the efficient trapping demands that the particle size should be several times smaller than the focal spot; besides, for suitable observations, the particles should not be very small compared to the radiation wavelength. And, finally, the tested particle should possess rather low absorption to avoid local heating with hardly controllable influence on the water's tribological parameters.

For all these conditions, weakly absorbing ($\kappa \lesssim 10^{-3}$) dielectric particles with diameter 0.5 to 2 μm are appropriate. Figure 3 demonstrates the spinning motion of trapped particles.

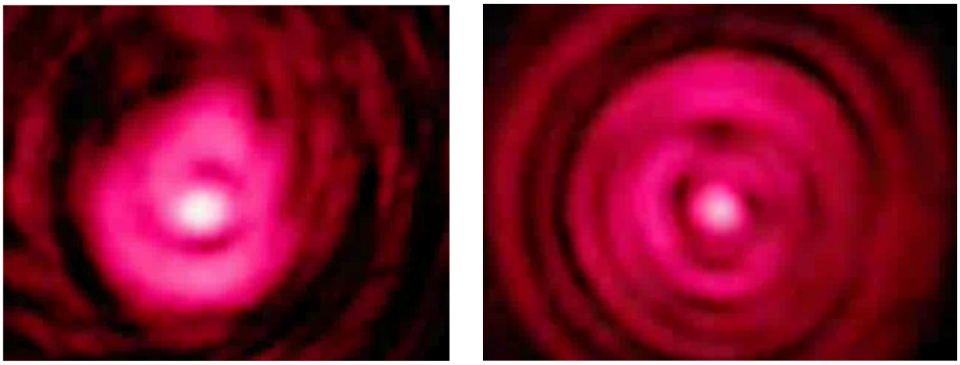

(a) (b)

Fig. 3. Video of the particle's spinning motion: (a) latex particle with Ren_p = 1.5, r = 0.5 μm, laser beam power 100 mW, see also in Media 1; (b) gamboge particle with Ren_p = 1.584, r = 0.4 μm, the beam power varying from 20 to 100 mW and back to zero, see also in Media 2.

Figure 3(a) shows rotation of a weakly absorbing latex particle illuminated by a beam with a stable maximum power 100 mW (initial laser beam ~140 mW). Gamboge particles of comparable size have noticeably higher absorption and spin with higher velocity (Fig. 3(b)). Besides, Fig. 3(b) clearly shows the spinning rate dependence on the laser beam power. A weak ellipticity of the particles' shapes facilitates observation of their spinning. By means of such videos, the spinning velocity can be easily determined with high accuracy (~1%). Its proportionality to the incident beam power expected from the theoretical considerations via Eqs. (5), (6) is confirmed by Fig. 4 which is derived from the data of Fig. 3(b).

#231377 - $15.00 USD Received 12 Jan 2015; revised 25 Feb 2015; accepted 25 Feb 2015; published 9 Mar 2015

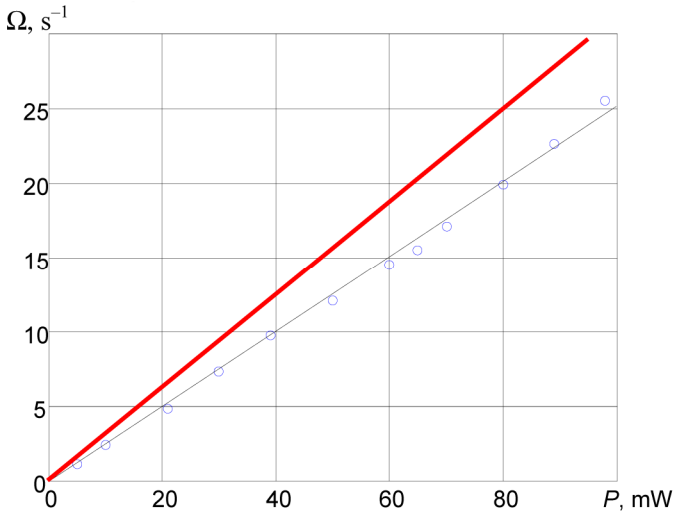

Fig. 4. Spinning rate of the gamboge particle of Fig. 3(b) vs the laser beam power: (markers) experimental data, (black) their linear fitting, (red) calculated by Eq. (5) for $n_p = 1.584 + 1.24 \cdot 10^{-3} i$, other conditions as in Fig. 3. The corresponding transition coefficient in Eq. (13) is presented in the 3rd row, 4th column of Table 1.

3. The method analysis and validation

To interpret the data obtained, note that the spinning motion is due to the field spin angular momentum absorbed by the particle and its angular velocity Ω is related to the radiation torque (5) by equality [20,21]

$$\Omega = \frac{T}{8\pi\eta r^3} \tag{12}$$

where η is the dynamical viscosity of the medium. Figure 5 presents the behavior of the absolute torque T and the angular velocity (12) as functions of the imaginary part of the refraction index κ for a particle suspended in water and trapped in the center of a focused Gaussian beam waist with radius w_0 = 2 μm and total power P = 100 mW giving an axial intensity of $I_0 = 1.59 \cdot 10^{13}$ erg/(cm^2·s). Calculations are performed according to Eqs. (5)-(7) and (12).

Figure 5 indicates a distinct relation between the particle spinning in a circularly polarized light and its absorption. Moreover, this relation is close to linear with a high accuracy, see the inset, which is favorable for many metrological practices because of potentially easy calibration and direct interpretation of the measurement results. In fact, the thick red line in Fig. 5 shows that the absorption index κ of the particle can be directly derived from the observed spinning velocity Ω exhibited by the particle in the beam with power P,

$$\kappa = q\frac{\Omega}{P} \tag{13}$$

where q is the transition coefficient. Assuming the Eq. (13) to be exact for $\kappa = 4 \cdot 10^{-4}$, we find $q = 4.37 \cdot 10^{-3}$ mW·s. Of course, this numerical value of the transition coefficient is only correct for the given beam and particle parameters specified above, and even the linear

#231377 - $15.00 USD Received 12 Jan 2015; revised 25 Feb 2015; accepted 25 Feb 2015; published 9 Mar 2015

character of the Ω–κ dependence is not obligatory true outside the considered range of the particle sizes and absorption indices.

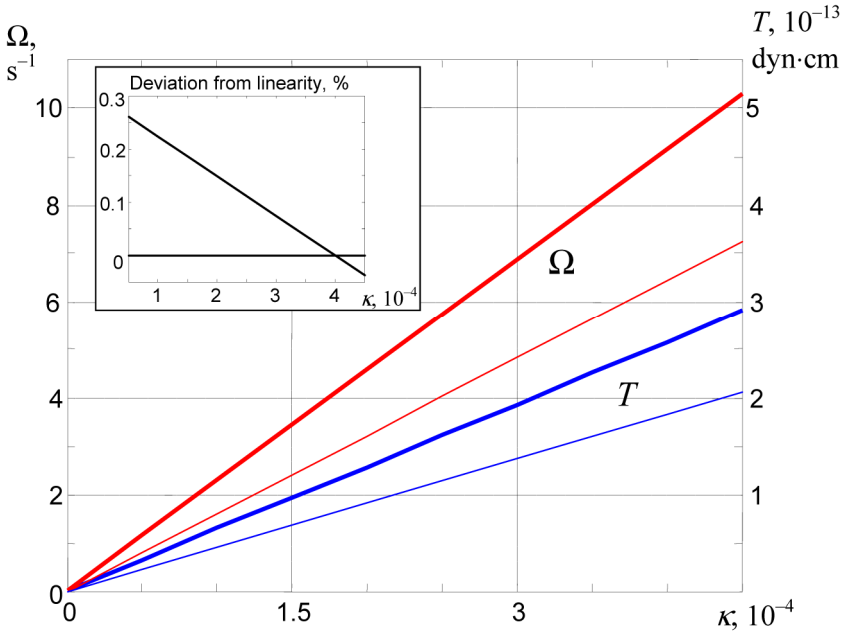

Fig. 5. Dependence of the (blue) radiation torque (5) and (red) corresponding angular velocity (12) of the spinning motion on the particle absorption index κ for a particle of radius r = 0.5 μm with μ_p = 1 suspended in water (μ = 1, n = 1.33, $\eta = 8.9\cdot10^{-3}$ dyn·s·cm^{-2}) and exposed to a circularly polarized Gaussian beam with wavelength λ = 0.65 μm (wavenumber in water $k = 1.286\cdot10^5$ cm^{-1}) and power 100 mW, focused into the spot with radius w_0 = 2 μm; thick (thin) lines correspond to the particle refraction index $n_p = 1.5 + i\kappa$ ($n_p = 1.2 + i\kappa$). Inset: relative deviation of the real Ω–κ dependence from the linear approximation (13)

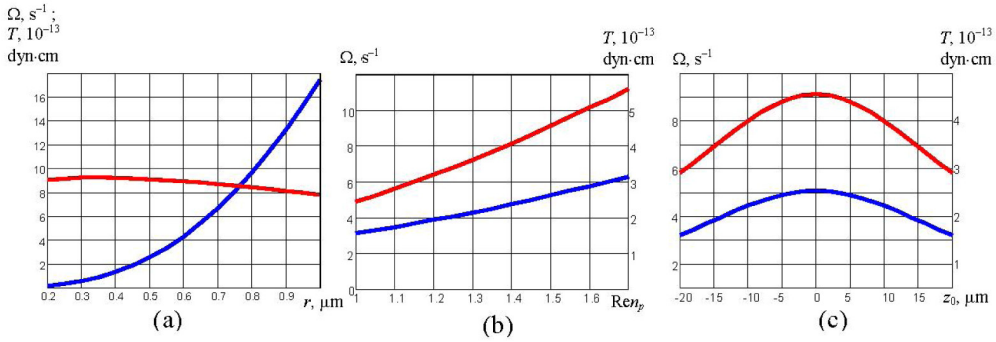

Fig. 6. (Blue) radiation torque and (red) corresponding angular velocity of the spinning motion of the particle with the absorption index $\kappa = 4\cdot10^{-4}$ suspended in water and trapped in the center of the Gaussian beam of Fig. 5: (a) Ren_p = 1.5, z_0 = 0, particle radius r is variable; (b) r = 0.5 μm, z_0 = 0, Ren_p is variable; (c) r = 0.5 μm, Ren_p = 1.5, z_0 is variable.

Now consider how the measurement efficiency can be affected by other factors which are not controllable as conveniently as the beam power P included in Eq. (13) or the beam waist size w_0. First note, the particle size is seldom known with high accuracy and even usage of mono-disperse powders for preparing the particle suspensions does not prevent random deviations in the diameter of any given particle from the nominal value. From this point, it

#231377 - $15.00 USD Received 12 Jan 2015; revised 25 Feb 2015; accepted 25 Feb 2015; published 9 Mar 2015

looks rather encouraging that, despite the strong variability of the absolute torque, the field-induced spinning velocity changes rather slowly (within units of percents) in the working range of the particle radii (0.3 – 0.7 μm), see Fig. 6(a).

Further, thin lines in Fig. 5 testify that, even though the optical torque appears as a selective sensor of particle absorption, its "sensitivity" generally depends on other optical parameters. In particular, one cannot recover the exact numerical value of the absorption index without knowledge of the real refraction index. In more detail, this feature is illustrated by Fig. 6(b), where it is seen that the ± 6% indeterminacy in n_p produces ± 10% inaccuracy of the absorption measurement.

It is important to note that for conditions of moderate focusing realized in our experiment, the particle cannot be optically stabilized in the longitudinal direction, i.e. there is no point where the z-directed radial pressure is compensated by the longitudinal gradient force "pulling" the particle back to the focal plane. This observation has been supported by the optical pressure calculation based on the Optical Tweezers Computational Toolbox [30]. Figure 6(c) illustrates possible variations of the spinning velocity owing to instability of the longitudinal position of the particle, which confirms that this can be a source of substantial errors. In our experiment, this difficulty is overcome by having a small longitudinal thickness of the cell (70 μm) where the floating particles are trapped at a certain distance from the back wall by hydrodynamic and photophoretic forces. Actually, each time a particle appeared to be trapped, its longitudinal position coincided with the waist plane with an inaccuracy not exceeding ± 10 μm, which, according to Fig. 6(c), may suppress the spinning rate up to 20%.

For the method verification and calibration, it should be applied to particles with known optical properties. To obtain such particles, we used the epoxy resin Epoxy DGEBA for two reasons: (i) this material allows generation of mono-disperse droplets with appropriate sizes without uncontrollable change of the chemical composition and physical properties [31] and (ii) it can be prepared in the form of a thin film whose optical constants can be easily measured by standard procedures. With the help of a spectrophotometer 6300 VIS and refractometer Atago NAR-1T Solid [32,33] we have found that for the wavelength λ = 0.65 μm, optical constants of Epoxy DGEBA resin are $\mathrm{Re}\, n_p = 1.572$, $\kappa = 6.0 \cdot 10^{-4}$.

These data are presented in the 1st row of Table 1. Knowing the particle's complex refraction index (4th and 7th columns of Table 1) and Gaussian beam parameters specified in the caption to Fig. 5, Eqs. (5) and (13) give the transition coefficient q and theoretical spinning velocity Ω_t = 14.8 s^{-1} (5th column). The measured value of the spinning velocity Ω_e = 12.2 s^{-1} (6th column) is rather close to the theoretical value although the difference of about 20% is not negligible. We associate this difference with the above discussed factors, first of all, longitudinal displacement of the particle z_0 (see Figs. 1 and 6(c)). An additional contribution

Table 1. Summary of the optical parameters and measured data for three sorts of particles trapped within the focused Gaussian beam with w_0 = 2 μm and P = 100 mW

1	2	3	4	5	6	7
Particle	r, μm	$\mathrm{Re}n_p$	q of Eq. (13), 10^{-3} mW·s	Ω_t, s^{-1} Equation (5)	Ω_e, s^{-1} measured	$\kappa = \mathrm{Im}n_p$, 10^{-4}
Epoxy DGEBA (calibration)	0.45	1.572	4.05	14.8	12.2	6.0
Latex	0.50	1.50	4.37	12.2	10.1	5.3
Gamboge	0.4	1.584	3.97	31.2	25.8	12.4

to this difference can be caused by a possible deviation of the cell temperature due to which the water viscosity exceeds the accepted value. Importantly, both reasons act similarly for particles of similar structure and physical nature; our experiments have shown that such a decrease of the spinning velocity as compared with the theoretical predictions repeats systematically and thus can be accounted for by the normalization coefficient v = 14.8/12.2 =

#231377 - $15.00 USD Received 12 Jan 2015; revised 25 Feb 2015; accepted 25 Feb 2015; published 9 Mar 2015

1.21. Confronting the theoretical Ω_t with the known value of κ (7th column, 1st row of Table 1), the transition coefficient $q = 4.05 \cdot 10^{-3}$ mW·s (4th column, 1st row) is derived from Eq. (13).

The normalization coefficient v facilitates a reduction in the measured data obtained for the other types of particles (2nd and 3rd rows of Table 1), to the "standard" conditions accepted for calculation of Fig. 5, i.e. the figures in the 5th column are just the data of the 6th column multiplied by 1.21. Corresponding transition coefficients of Eq. (13) are calculated by means of Eq. (5) and given in the 4th column. After substitution of Ω_t and q into Eq. (13), one easily finds the absorption indices presented in the 7th column, which completes the measurement procedure. The self-consistency of this result is confirmed by the red line in Fig. 4 that, being theoretically calculated for $n_p = 1.584 + 1.24 \cdot 10^{-3} i$, practically describes the data of the black line (experiment) multiplied by v.

Conclusion

In this work we describe a special approach, based on light-induced particle spinning, which enables directly measuring the light absorption of microparticles. Despite that it involves rather exquisite technical means including optical trapping and manipulation, an intensive development of such practices in the past years makes the proposed method available and attractive for many laboratories. Moreover, it is quite expectable that the study of mechanical motion of microparticles trapped within an optical field offers a lot of new interesting possibilities for metrology of their optical properties making the present paper a first step in this direction.

In the present form, the approach is rather specialized and aimed at determining the particle's absorption provided that other optical parameters (e.g., real part of the refraction index) are known. Such a situation is typical for weakly absorbing dielectric particles where doping or small variations of the chemical composition can noticeably modify the absorption parameters leaving the refraction index practically unchanged. More importantly, the relation between the particle spinning motion and its absorption index is immediate and not contaminated by irrelevant contributions as might be the case if the absorption characteristics had been derived from the optical force data regulated by the 'total' imaginary polarizability (6). An additional benefit of this method is the linear character of the indicative dependencies (Fig. 5) which offers suitable calibration options for any practical implementation. Of course, this linearity is only preserved for small absorption ($\kappa \sim 10^{-3}$ or less) but this is just the typical condition for doped dielectric particles.

Important questions emerge on the limits of absorption that can be measured by this method. Generally, there is certain flexibility associated with the particle's refraction and the choice of driving beams with necessary power and degree of focusing. However, rough estimations can be made, grounding on Eq. (13). Indeed, the coefficient q depends on the beam and particle parameters but, in all cases, its order of magnitude will not differ substantially from what was accepted in Section 3 and Table 1. The lower limit of the detectable rotation velocity is restricted by natural instabilities of the particle position and orientation caused by stochastic influences; let it roughly be 0.1 s^{-1}. Reasonable maximum of the beam power, in view of possible self-induced effects in the suspending medium [7], may be taken 1 W, and then the minimum measurable absorption index appears to be $\kappa \sim 4 \cdot 10^{-7}$. If the particle is suspended in a less dense medium, this limit can be overcome; for example, in air with viscosity $\eta = 1.8 \cdot 10^{-4}$ dyn·s·cm^{-2} [21], the minimum measurable absorption goes down to $\kappa \sim 10^{-8}$. The upper limit can be determined by the conditions that the absorbed energy does not change the medium's tribological parameters and is homogeneously distributed over the particle volume; both requirements lead to conclusion that reliable results can only be expected while $\kappa \leq 10^{-2}$. Of course, in real situations, proper optimization procedures can noticeably improve our present speculations.

#231377 - $15.00 USD Received 12 Jan 2015; revised 25 Feb 2015; accepted 25 Feb 2015; published 9 Mar 2015

Evaluation of the method's accuracy is somewhat hampered by the spread of the data on the particles' absorption available in the current literature. However, even in its simplest form described here, the method demonstrates rather high sensitivity and good prospects for the accuracy improvement, associated with due calibration and stabilization procedures. It is to be expected that a proper control of the beam power in the cell, the cell temperature, the suspending medium viscosity and the particle longitudinal position will make the proposed method a suitable way for investigation of weakly absorbing particles.

Acknowledgments

Steen G. Hanson acknowledges the financial support from the Danish Council for Technology and Innovation under the Innovation Consortium LICQOP, grant #2416669.

#231377 - $15.00 USD Received 12 Jan 2015; revised 25 Feb 2015; accepted 25 Feb 2015; published 9 Mar 2015